Electromagnetic Emissions from PPS®1350 Hall Thruster

IEPC-2009-071

Edward J. Beiting, Xuan Le Eapen, James E. Pollard
The Aerospace Corporation
P.O. Box 92957 – M2/341
Los Angeles, CA 90009-2957

Marc Gambon, Frédéric R. Marchandise, Michael Öberg
SNECMA, Division Moteurs Spatiaux
Site de Vernon, B. P. 820
27208 VERNON, FRANCE

Measurements were taken on two nearly identical PPS1350-G EM Hall thrusters with BOL and EOL accumulated operating hours. Spectral scans of radiated electric fields were recorded from 10 kHz to 18 GHz following MIL-STD 461E RE102 specifications and from 18 to 32 GHz with a 1 MHz (3 dB) bandwidth. As is typical for Hall thrusters, emission exceeded the MIL-STD 461E limit at all frequencies below 300 MHz and between 900 and 2000 MHz for both antenna polarizations when the thrusters were operating in their normal mode. Emission in the 1 – 8 GHz spectral region was less than that seen previously from similar thrusters. Time domain measurements under steady-state thruster operations were made for nine operating points for each thruster. These measurements employed a four-channel instrument that individually and simultaneously viewed the entire L-band, S-band, C-band, and the partial X-band (7.9–8.4 GHz). A second instrument, operated in parallel with the LSCX instrument, sequentially recorded emission at one of ten frequencies with a 50-MHz bandwidth. The pulsed radiation from these data was reduced and is presented as distributions of pulse frequency versus amplitude to permit quantitative estimates of increases in receiver noise temperature or bit error rates. Transient effects were also recorded using these time-domain instruments. Emission was taken during thruster startup with 5 μs temporal resolution; this radiation could exceed the steady-state emission by two orders of magnitude (40 dB). Other transient measurements observed emission change during an increase in anode voltage, a decrease in magnetic field current, and an increase in pressure to the inlet manifold of the xenon flow controller (XFC).

Nomenclature

BOL	=	beginning of life
CNES	=	Centre National d'Etudes Spatiales (French national space agency)
DAQ	=	data acquisition
DSO	=	digital sampling oscilloscope
EOL	=	end of life
EMC	=	electromagnetic compatibility
FU	=	filter unit
HET	=	Hall effect thruster
LNA	=	low noise amplifier
LSCX	=	time domain instrument that covers L, S, C, and partial X-band in four channels
OP	=	thruster operating point
MIL-STD	=	Military Standard
PPU	=	power processing unit
RBW	=	resolution bandwidth
XFC	=	xenon flow controller
XRFS	=	xenon regulation and feed system
Zspan	=	zero span (non scanning) operation of spectrum analyzer

I. Introduction

It is well known that Hall effect thrusters (HETs) emit significant electromagnetic radiation from DC (static electric and magnetic fields) to frequencies above 20 GHz.[1-4] This emission varies with HET type and as a function of operating point for a specific thruster. In principle, after a general characterization of emission is completed for all operating points of a thruster, more detailed studies should be undertaken with the particular requirements of a payload taken into consideration. Interestingly, previous studies of this kind have found both direct[5] and indirect[4] evidence that emission in important communication bands can increase for some HETs as a function of accumulated operating hours. The work presented here was undertaken to investigate these phenomena for the PPS®1350 Hall thruster.

This paper presents measurements of radiated electric fields from two PPS®1350 Hall thrusters provided by SNECMA (a PPS1350 MIr and a PPS1350-G EM). These thrusters were chosen to be nearly identical except for age. Because of this age difference, they exhibited distinct levels of oscillation and emission (see ref. 6 for age-related oscillation of the PPS1350). The measurements were part of thruster qualification campaign funded by CNES-SNECMA and the data presented here is only a few percent of the of the large emission data set taken at The Aerospace Corporation during this campaign.

Radiated emissions were recorded from these thrusters for nine operating conditions. The measurements included (1) radiated electric fields from 10 kHz to 32 GHz following MIL-STD 461E RE102 specifications for the principal operating condition; (2) L-, S-, and C-band spectral scans to identify changes in emission as a function of thruster temperature and operating condition; (3) steady-state time domain medium bandwidth (50 MHz) and broadband (> 1 GHz) emission in the L-, S-, C- and X-bands; and (4) transient electric field emission during thruster start-up, a magnetic field decrease, an anode voltage increase, and an increase in inlet pressure to the XFC for different thruster operating points. A description of the thrusters and their operation are presented in section II, the facility and its characteristics are given in section III and the principal results are described in section IV. Section V is a short summary with conclusions.

II. Thrusters and Their Operation

The PPS®1350-G is a thruster adapted for North/South station keeping of satellites in the range 1 to 4 tons in Geostationary Earth Orbit (1.7 to 6.5 tons in GTO). It has a nominal operational point (U= 350V, I = 4.28A) chosen to deliver 88 mN with 1500 W of electrical input power. The characterization of the PPS®1350-G thruster in terms of radiated EMI emissions was based on two thruster units: The MIr model (PPS-1350) was used to achieve the Stentor life test qualification (see Figure 1) and the Engineering Model (EM), having the same configuration of that of the QM model, to demonstrate EMI/EMC compliance. The only difference between the PPS1350 and PPS1350-G configuration is the material chosen for the anode xenon distribution ring and the back cover plate that was simplified for the PPS1350-G. The PPS1350 MIr was equipped with a stainless steel anode to have a closer similarity to the PPS1350-G. Thus, the functional parts are identical and in particular, the magnetic configuration, geometry of the chamber and the anode, the material of the chamber, and thermal inertias of the functional part are not modified between the PPS®1350 and the PPS®1350-G.

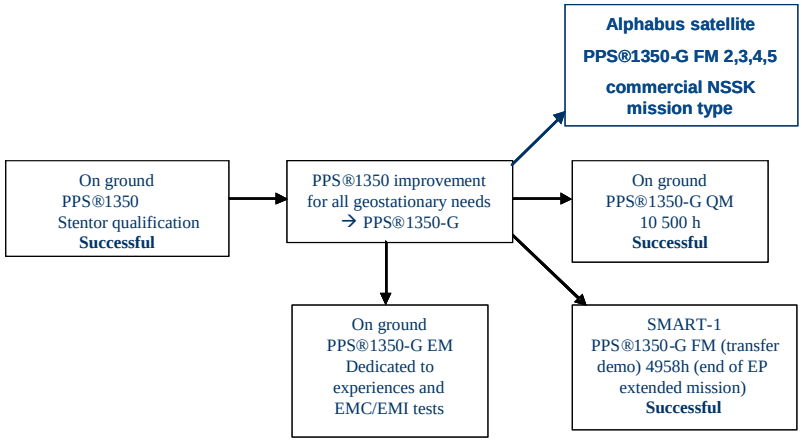

Figure 1. The PPS®1350-G qualification process.

As noted above, the principal difference between the thrusters used for these studies was their accumulated operating time. In particular, the EM is a thruster at BOL and the MIr is a thruster nearly at EOL. Table 1 presents the two PPS®1350-G thruster models life test history prior to the radiated EMI characterization.

Table 1

PPS®1350-G Thruster	Accumulated Cycles and Hours prior to EMI testing	Accumulated Cycles and hours during EMI testing
MIr	5740 cycles / 6450 hours	51 cycles / 50 hours
EM	100 cycles / 200 hours	35 cycles / 45 hours

The Aerospace Corporation built a system that operated the PPS1350-G thruster in a manner that emulated the flight-model PPU and XRFS. Top-level functions included automated thruster start sequences, running at nine different operating points, closed-loop control of discharge current via the XFC thermo-throttle, and XFC inlet pressure pulses to represent the flight-model XRFS behavior. The system was operated using LabVIEW® programs for commanding the hardware, for recording thruster and facility telemetry, and for safely shutting down in the event of a fault condition.

Input power for the PPU electronics was via isolation transformers. Each power supply chassis (with the exception of the igniter supply) was connected by a wire having less than 30-mohm resistance to a star point in the PPU rack. The star point was connected to an isolated earth ground by a cable having a 0.7-mohm resistance. There were no hard-wired connections from any PPU chassis to the vacuum chamber or to a non-isolated structure ground. Each power supply output terminal (again with the exception of the igniter supply) was internally isolated from its chassis. The PPU relied on commercial switching-type supplies (Lambda GEN series) except for the igniter, which was a custom-built pulse generator on loan from Snecma. A switching-type anode supply (GEN600-8.5) was used for the majority for the testing, but a linear-type supply (EMHP 600-50) was used for a small set of comparative measurements. Unlike the other supplies, the pulsed output of the igniter was referenced to its chassis, which was floated at the cathode reference potential. Uninterruptible power was provided for all PPU electronics except for the anode and igniter supplies.

The propellant was supplied to the thruster and cathode by a custom-built xenon regulation and feed system (XRFS) that was versatile enough to mimic the output pressure transients of an Astrium flight model XRFS[7]. Both the PPU and XRFS were controlled and monitored by computer. The nine thruster modes used in this study are identified in Table 2.

Table 2 Parameters for the Nine Thruster Operating Points

Operation Point (Mode)	Discharge Volts	Anode Current (A)	Power Watts	Magnetic Current Im (A)	Propellant Flow (mg/s)	Corrected Pressure (mbar)
OP1	350	4.28	1500	0	5.45	2.36E-05
OP2	350	4.50	1575	0	5.73	2.48E-05
OP3	350	3.40	1190	0	4.33	1.87E-05
OP4	300	3.00	900	0	3.82	1.65E-05
OP5	265	2.50	660	0	3.18	1.38E-05
OP6	220	2.10	460	0	2.67	1.16E-05
OP7	300	5.00	1500	0	6.37	2.76E-05
OP8	350	4.28	1500	1.75	5.45	2.36E-05
OP9	250	4.28	1070	0	5.45	2.36E-05

Thruster operating parameters were recorded in parallel to the radiated EMI measurements. The static and dynamic behavior of the anode discharge current was recorded via a current probe to observe the oscillations present just upstream of the thruster. The current probe was mounted between the thruster and the filter unit, placed 1m electrically upstream of the thruster. The current probe had a bandwidth of 120 Hz – 20 MHz, -3dB. The discharge oscillations were recorded, processed and analyzed on a DSO. These parallel measurements as well as time-domain emission measurements made by CNES are not reported in this paper.

III. Facility

The Aerospace Corporation's EMC facility is shown in Figure 2. A small (0.9 m diam. and 1.5 m long), all-dielectric vacuum tank houses the thruster. This fiberglass tank is largely transparent to electromagnetic radiation and mates to a stainless steel vacuum chamber, which is pumped with four cryotubs and four reentrant cryopumps. The tank is constructed of S2 glass. A high-power thruster placed in this chamber is usually mounted on a water-cooled plate to control its temperature. All bolts, fittings, water lines, flanges, and support fixtures within and attached to the fiberglass tank are fabricated of electrically non-conducting materials. A more complete description of the characteristics of the dielectric tank is available[8].

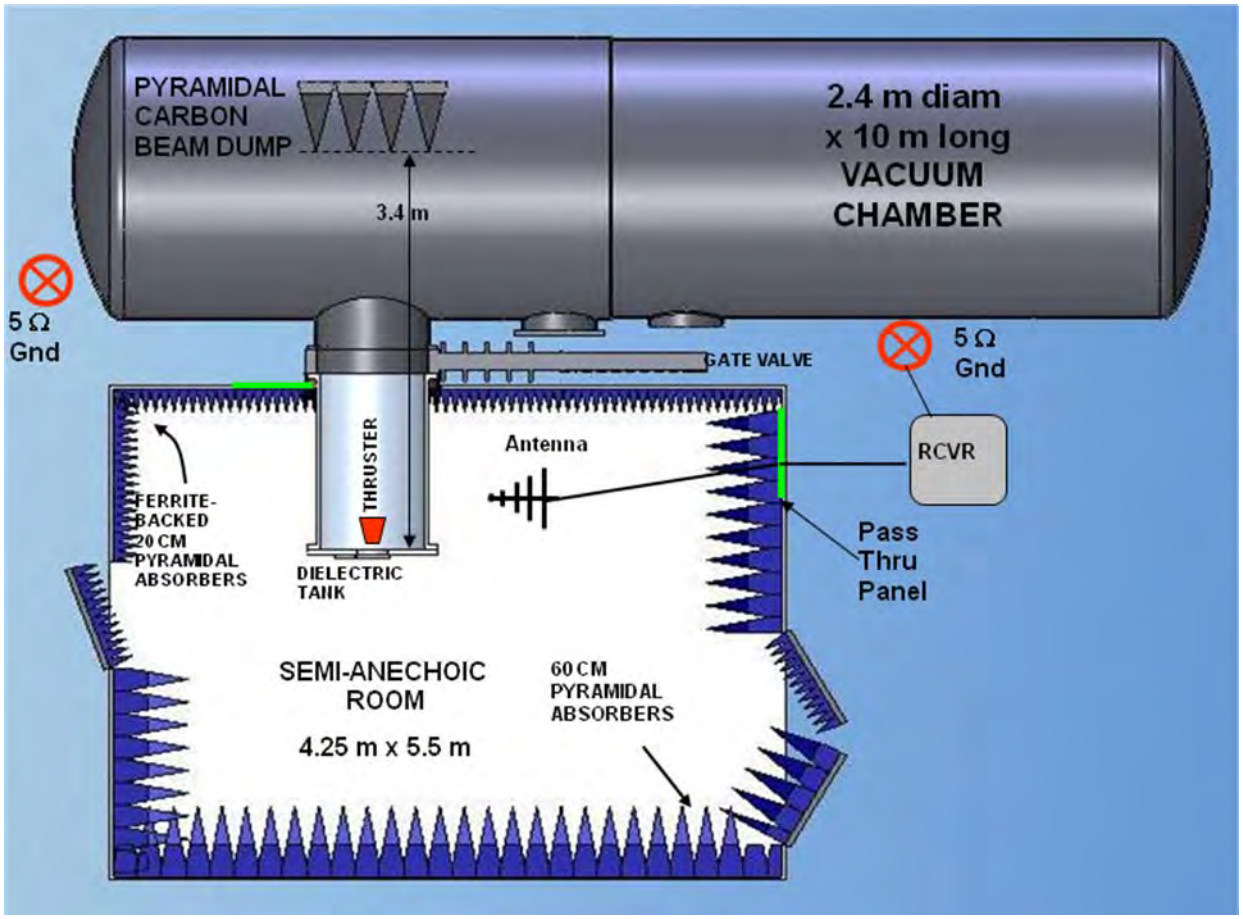

Figure 2. Scale Drawing of The Aerospace Corporation's EMC Facility.

The small tank size allowed antennas to be placed sequentially outside the vacuum to the side the thruster at a distance of one meter from the thruster as required by MIL-STD 461E. This geometry precludes the possibility of antenna-plasma and antenna-antenna interaction. Ambient radiation leaks into the main vacuum tank through openings and cables attached to equipment in the tank. Subsequently, this radiation leaks into the anechoic room through the fiberglass tank orifice and is especially apparent in the 20–200 MHz frequency band, where there is room resonance (see background traces in the data figures in Section IV). In most cases this radiation was at least 10 dB below the measured signal.

A 5.5m x 4.25m x 3m semi-anechoic room, surrounds the dielectric tank to shield the thruster from the ambient electromagnetic environment. It provides >100 dB shielding from 14 kHz - 18 GHz and is designed to be MIL-STD 285 and NSA 65-5 compliant. The plume of the thruster exhausts into the main vacuum tank, terminating on a beam dump comprising a series of 0.6-m-high aluminum pyramids covered with grafoil to reduce sputtering by the high-energy xenon ions and reduce scattering of electromagnetic radiation from the thruster by main tank at higher frequencies. Two panels allow cables from antennas and

thruster service lines to exit the semi-anechoic room along the ground plane. A complete description of this facility, including performance measurements, is available in a recent paper[9].

The final component comprises the calibrated systems (analyzers, receivers, and custom-built time-domain instruments) that record the radiation emanating from the thruster. Below 18 GHz, the instruments connect sequentially to a series of antennas through a panel in the semi-anechoic room using a two-section semi-rigid cable with known attenuation. Above 18 GHz, a smaller receiver situated in the anechoic room connects sequentially through one of two short cables to a series of low-noise amplifiers (LNAs) and octave horns. The antenna position used in these measurements was 1 m to the side of the thruster, closest to the side-mounted cathode, as shown in Figure 3.

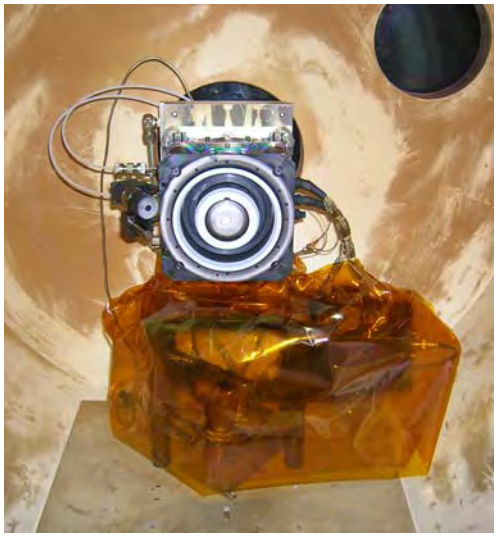

Figure 3. Photograph of PPS1350-G EM mounted in fiberglass tank. The cathode is mounted to the left, closest to the antenna placement.

A photograph of the PPS1350-G EM in the fiberglass tank is presented in Figure 3. The thruster was attached to a vertical aluminum bracket that was backed with a 152 x 203 mm (6" x 8") water-cooled plate, positioned so that the centerline of the thruster coincided with the centerline of the fiberglass tank. The water-cooled aluminum plate remained below 25^{o}C for all operating conditions. Propellant lines were routed along the bottom of the dielectric chamber underneath a fiberglass plate (shown at the bottom of Figure 2-2) to vacuum feedthroughs in the main chamber.

Only two of the eight cryopumps were operated while measurements were made, resulting in a measured xenon pumping speed in the main chamber of 41,000 liter/s. The effective pumping speed in the fiberglass chamber was approximately 20,000 liter/s in this configuration. The expected flow rate for OP1 was 5.45 mg/s. A value of 5.23 mg/s was observed for OP1; the difference was likely due to back-ingestion of xenon in the conductance-limited fiberglass chamber. The corrected pressure (0.348 that of the measured pressure) was 2.36 x10^{-5} mbar in the main chamber when the thruster operated in OP1. The flow rate and background pressure scale with the anode current. The scaled values for these quantities are given in the last two columns of Table 2 for the nine thruster operating conditions.

IV. Radiated Electric Field

Spectral Measurements

Complete MIL-STD 461E RE102 spectra were recorded for the PPS1350 MIr and the PPS1350-G EM thrusters for OP1. A composite set of spectra over all bands from 10 kHz – 18 GHz for both thrusters and antenna polarizations is presented in Figure 4. Care should be taken in comparing the vertical and horizontal polarizations in these plots, as the frequency scales are considerably different for the two panels. The background shown in green is 10 dB or greater below the signal levels, and hence does not contribute significantly to the signal trace on these log-log plots. The 50 Ω load line trace indicates the sensitivity of the instrumentation.

With the exception of the large vertically polarized emission near 32 kHz (which originates from the fundamental breathing frequency of the thruster), below a frequency of 1 GHz the emission from the MIr thruster is consistently higher than that from the EM thruster. Because the thrusters are essentially identical except for age, one may attribute this increased emission with increased thruster operating hours. In the frequency interval between 10 and 500 MHz, this increase is between 10 and 20 dBμV/m. This sub-GHz emission, which originates from main discharge plasma modes as is discussed in detail elsewhere[10], follows the general pattern seen in both the SPT-100 and the BPT-4000 HCTs within ±10 dB.[3,4]

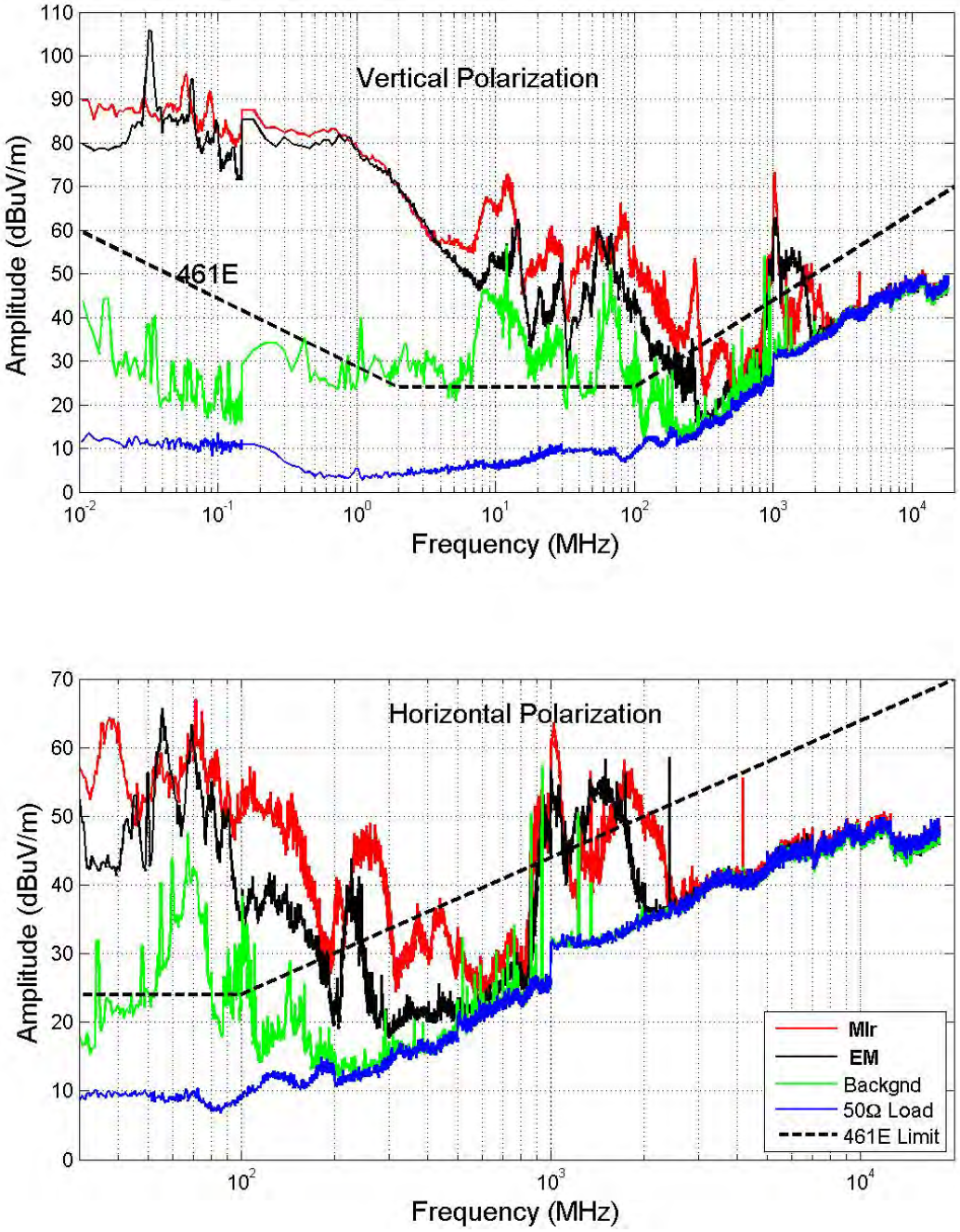

Figure 4. Spectra from 10 kHz–18 GHz (vertical polarization, upper panel) and 30 MHz – 18 GHz (horizontal polarization, lower panel) for the PPS1350 MIr and the PPS1350-G EM thrusters.

Above 1 GHz, however, the emission from the PPS1350 is substantially less than that seen previously from either the SPT-100 or the BPT-4000 thruster. The 1-8 GHz emission from the SPT-100 has been

studied extensively[4,5,11-13] and there is evidence that this L-, S-, C-band emission increases with thruster age. This substantial and increasing emission motivated much of the study here. A 1000 hour study monitoring the L-, S-, C-band emission from the BPT-4000 HCT, however, showed no increase in this emission with thruster age.[3] A recent study of this emission found the L-band (1-2 GHz) radiation was associated with the cathode only whereas the S- and C-band radiation was associated with the main plume and possibly its interaction with the cathode plume.[14]

The dissimilarity of this emission between the PPS1350 and the SPT-100 is surprising given the design similarity of the two thrusters. The two principal differences between the PPS1350 with the SPT-100 thrusters that could lead to such a difference is the cathode plume-thruster plume angle and a difference in the magnetic field gradient. Recent studies at The Aerospace Corporation using a different HET[15], indicate that the cathode position is unlikely to cause this different in emission but that characteristics of this emission are quite sensitive to the magnetic field. Indeed, the first eight operating points of this listed in Table 1 cause significant variations in this emission. None of these variations, shown in Figure 5, give rise to emissions as large as seen in the SPT-100. The origin of this emission is still an area of active research.

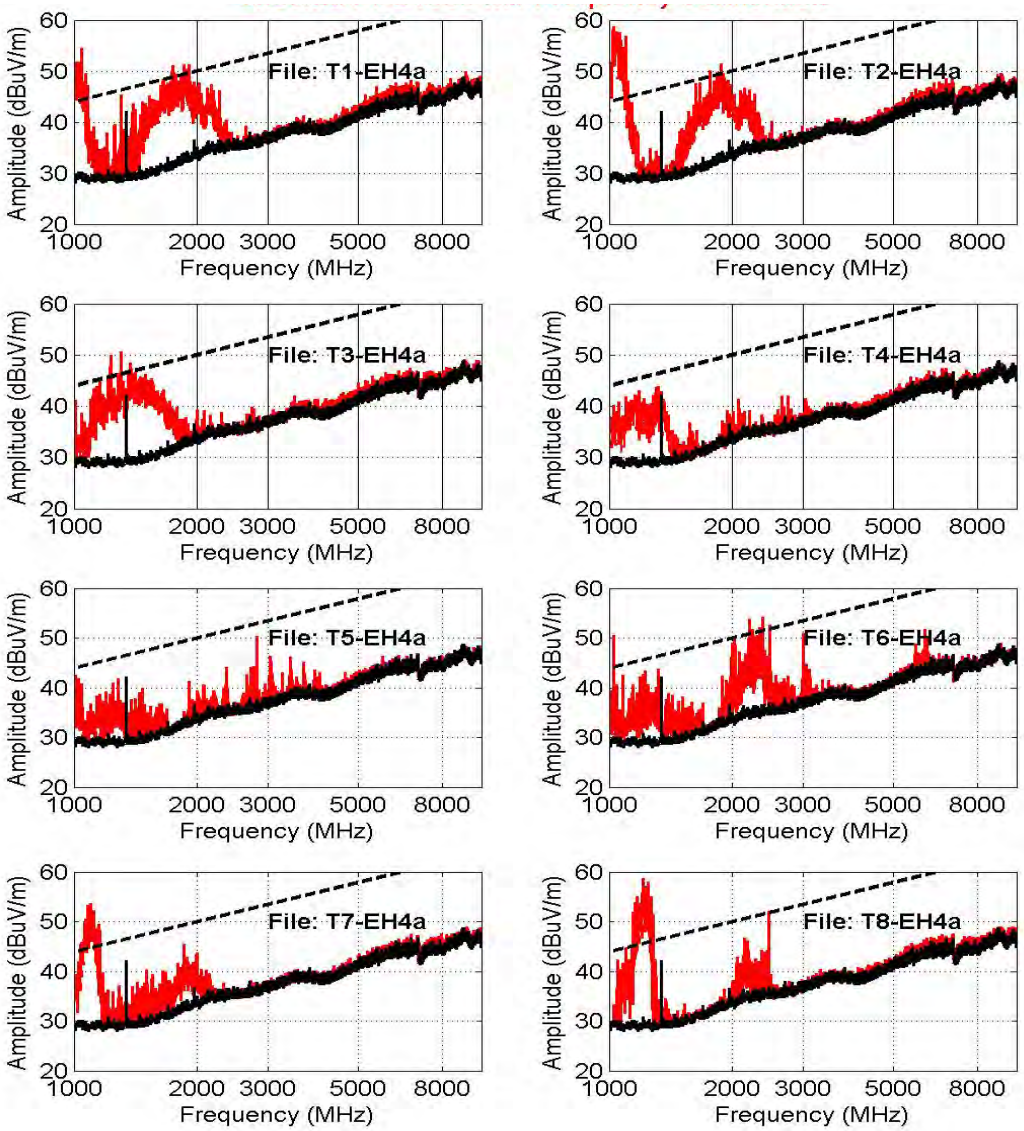

Figure 5. Variation in the spectra as a function of operation mode for OP1–OP8 for horizontal polarization and the PPS1350-MIr thruster. Blank curve is thruster off; red curve is thruster on, dashed line is MIL-STD-461 limit.

Above a frequency of 18 GHz there is a difference between the emission seen from the BPT-4000 and the PPS1350 (above 18 GHz, the emission from the SPT-100 has not been studied.) The BPT-4000 shows electron plasma frequency emission up to 22 GHz, especially for the high power (4.5 kW) high discharge voltage (400V) operating mode.[2] The frequency of this emission scales with the square root of the electron density. This result indicates that the maximum electron density in the plume of the PPS1350 is less than that in the BPT-4000. The lack of emission above background levels in the 18–32 GHz frequency range is show in Figure 6, which indicates the sensitivity of the measurement.

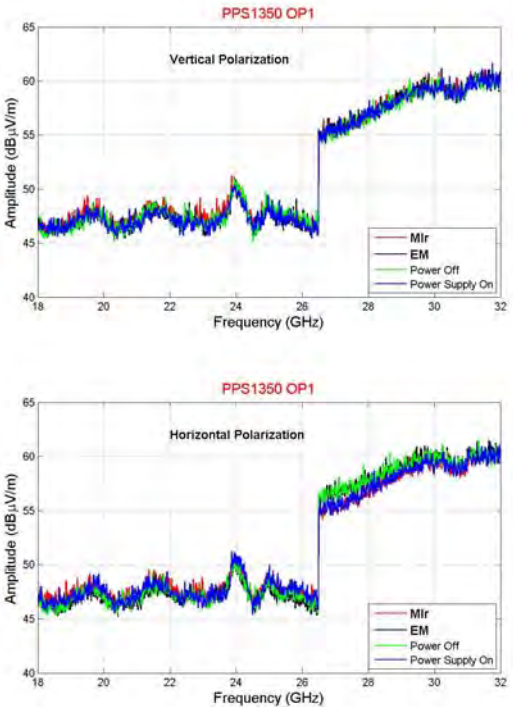

Figure 6.. Spectra from 18 kHz–32 GHz (vertical polarization, upper panel, horizontal polarization, lower panel) for the PPS1350 MIr and the PPS1350-G EM thrusters

Time Domain Measurements

Two custom-built time domain instruments were assembled for these studies. A broadband instrument (the LSCX instrument) comprised four broadband channels encompassing the entire L-, S-, C-bands and the 7.9-8.4 GHz region of the X-band. Each channel included a filter, two low-noise amplifiers (LNAs) separated by a (variable) attenuator, and a broadband detector (see Figure 7). The value of the attenuator was adjusted to accommodate the signal level in the channel to assure that the strongest pulses encountered during a measurement did not saturate the second LNA. The output from each component train was sensed by one of the four channels on a Tektronix 3054 digital sampling oscilloscope (DSO) using the peak sampling mode. In this mode, only the greatest amplitude that appears on the DSO input during any of its (10,000) sampling intervals is recorded.

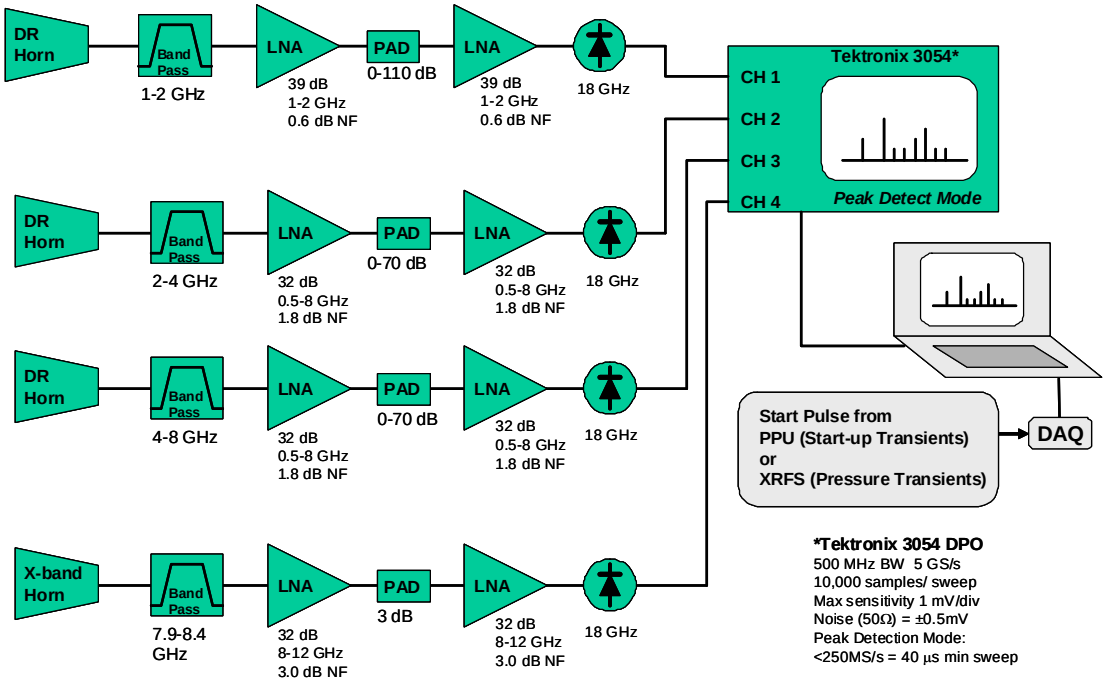

Figure 7. The LSCX TD instrument

Because the channels of the LSCX instrument had large bandwidths (500–4000 MHz), a second instrument, shown in Figure 8, which had a RBW of 50 MHz was used to acquire time-domain data with greater frequency specificity sequentially at 10 frequencies of interest. In order to maximize the sensitivity of the instrument, a separate antenna was used for each channel rather than splitting the signal from a single antenna to multiple channels. Accordingly, data were acquired simultaneously for the six instruments (including the Zspan and CNES instruments) using a plastic structure to precisely point six horn antennas to the same location 1-meter from the antennas.

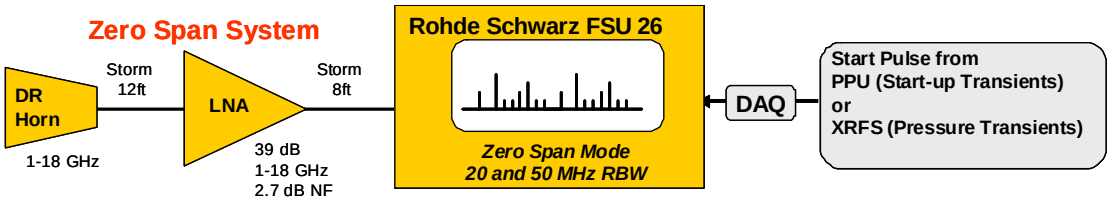

Figure 8. The Zspan time domain instrument.

There are many ways to reduce the data from these instruments, of which the method illustrated here represents one. Figure 9 shows one example of the more than 100 plots taken of the vertically polarized emission taken with the four channels of the LSCX instrument from the PPS1350-G EM thruster operating in OP6. These were a result of ten 10-second scans for a total of 100 seconds of data. On the left side of the figure the voltage registered by the DSO is converted to log electric field. The ten scans are concatenated and the result is plotted as a function of time.

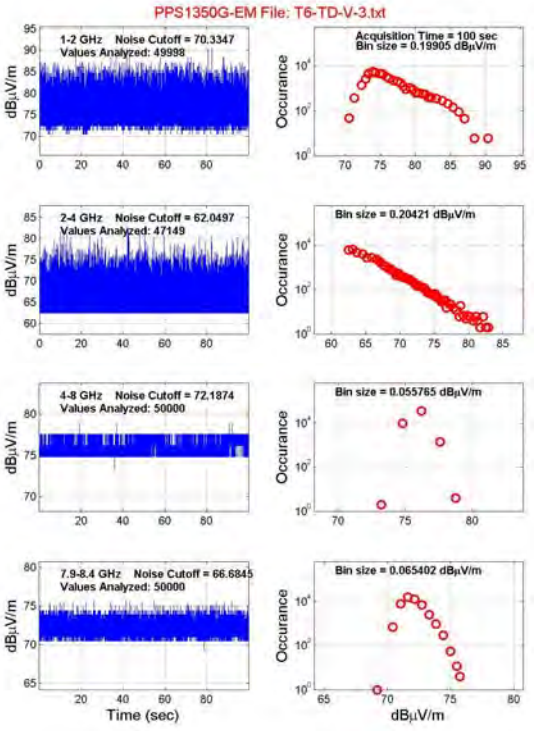

Figure 9. Log plots of 10 seconds of LSCX time domain data for the PPS1350-G EM operating in mode OP6. The left-side plots are the log amplitude electric field pulses; the corresponding right-side graph plots the distribution of these pulses

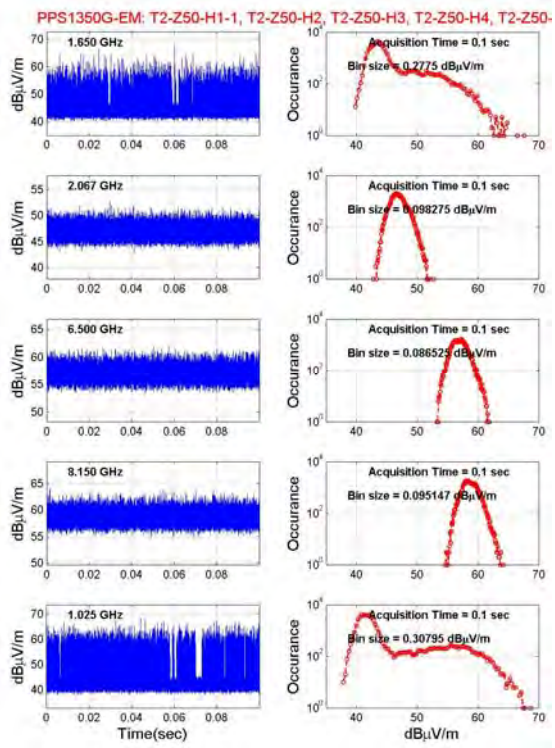

Figure 10. Log plots of 100 ms of zero span time domain data for five of the ten frequencies taken in horizontal polarization for the PPS1350-G EM operating in mode OP2. The left and right side panels are the same as those in Figure 9.

On the right side of the figure, the calibrated amplitude values above a specified level (listed on each plot) are sorted into amplitude bins and plotted as a histogram. If these histograms were due to only the thermal noise of the instrument, they would be symmetric Gaussian distributions similar to that seen in the X band distribution in the bottom right panel. The long tails on the high amplitude (right) side of the distribution are due to the emission from the thruster. (Because the low amplitude thermal pulses are omitted from the plots to speed the processing time, the peak of the thermal distribution may not appear.) These plots show a high rate of emission in the L and S bands but little emission in the C and X bands, which is consistent with the spectral plot for OP6 panel in Figure 5.

Figure 10 shows one example of the more than 200 figures of log plots of steady-state zero-span time domain data taken. Each figure displays five of the ten frequencies taken at a given antenna polarization and operating point for each thruster. In this figure, 100 ms of emission from the PPS1350-G EM operating in mode OP2 is presented in the same format used for the LSCX time-domain data. That is, the left side shows the log amplitude plots of electric field pulses and the corresponding right side plots the distribution of these pulses. In these distributions, the second, third, and fourth plots show symmetric Gaussian distributions, clearly indicating that only thermal instrument noise was recorded at these three frequencies in the 50 MHz resolution bandwidth. The first and last plots, however, show the emission from the thruster at these two frequencies as long tails to the right (high amplitude) side of the Gaussian thermal peaks. By summing the number of pulses in each bin above an amplitude level of concern, one may predict the increase in bit error rate (BER) in a receiver of known characteristics.

Transient State Time-Domain Measurements

Three types of transient time-domain measurements are described in this subsection. They are emission during (1) a cold thruster start-up, (2) a decrease in magnetic field for OP8 operation, and (3) an increase in anode voltage (250 V to 350 V) during OP9 operation. Each is discussed briefly in this order.

Start-up emission was recorded for OP1 and OP9 for the PPS1350 MIr thruster and for OP1, OP8, and OP9 for the PPS1350-G EM. Scans of 50 ms duration were taken producing a temporal resolution of 5 μs. The four channels of data from the LSCX instrument and one channel of data for one frequency of the Zspan instrument were taken concurrently. The Zspan data were acquired sequentially at three frequencies (1.65, 2.0675, and 6.50 GHz) so there where three LSCX data sets for each frequency (two polarization) set of Zspan data. This allowed a small statistical sample to observe start-up to start-up variations in the LSCX data. All start-up data were taken when the thruster was at or below a temperature of 25^{o}C. Examples of the LSCX and Zspan startup data are presented in Figures 11 and 12, respectively.

Figure 11 displays horizontally polarized OP1 startup emission from the PPS1350 MIr thruster. This startup registered emission in all four bands. Most startups did not show this high level of emission, and emission in the X-band channel is unusual. Examining complete data set, the start-up emission looks to be larger for the PPS1350 MIr thruster than the PPS1350-G EM thruster for the limited number of startup samples taken. Observations of startup bursts of the emissions in the LSCX bands showed in some cases levels 25-35 dB higher than at steady state conditions.

Figure 12 shows an example of Zspan startup emission from the PPS1350-G EM thruster in both polarizations for the three chosen frequencies. It should be emphasized that in contrast to the LSCX data, the emission shown in the six panels in this figure were taken with six different thruster starts and their amplitudes cannot be correlated. The transient amplitudes registered in these data are considerably higher than those measured in steady-state operation. In general, the maximum peak emission during the start transients of the PPS1350-G lasted for 5-10 msec, with levels approximately 25-35 dB higher than the steady state levels.

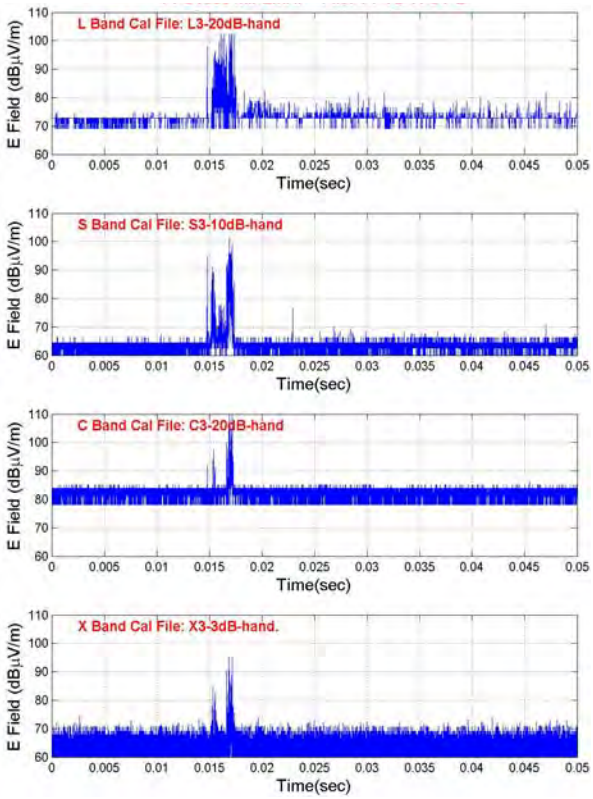

Figure 11. Log plots of horizontally polarized electric field emission from LSCX TD showing 50 ms of startup data from the PPS1350 MIr thruster. All in this panel data were taken with one thruster start.

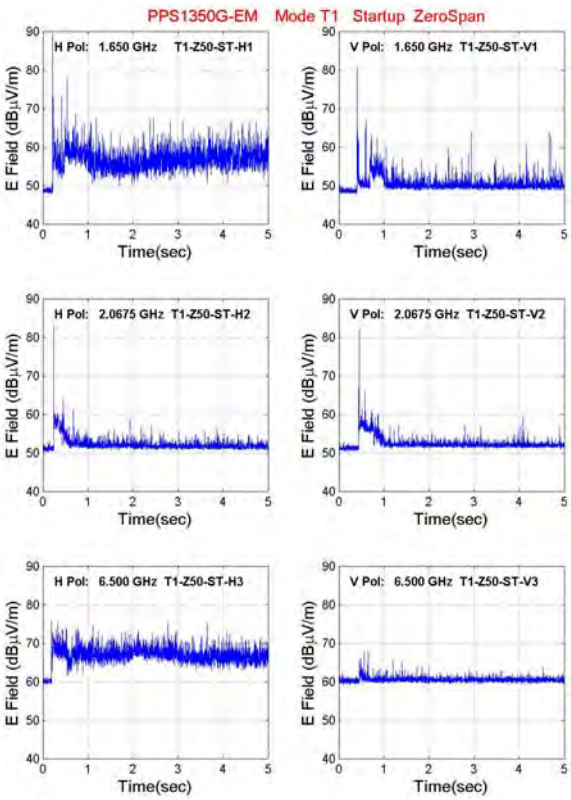

Figure 12. Log plots of zero span time-domain emission from the PPS1350-G EM thruster for three frequencies and two antenna polarizations. The emission in each panel in this figure was taken with a different thruster start.

Measurements of E-field emission during magnetic field transients were taken 15 minutes after thruster start-up for both thrusters. A timing pulse was sent to the EMC data acquisition systems 1 sec before the transient; data were acquired for a 2 sec duration, placing the emission change (if any) near the center of the scan. Figure 13 shows the horizontally polarized electric field emission from the PPS1350-G EM thruster taken with LSCX instrument. All data shown in this figure were taken with one transition. The change in emission near 1 sec in the L and S band panels is due to a drop in the magnetic field. No significant change in emission is observed in the C and X bands. The Zspan data for the OP8 magnetic transient did not show significant changes in emission for the three frequencies chosen.

Figure 14 provides an example of the Zspan data for the PPS1350 MIr thruster acquired during the anode voltage ramp. Here data in each of the six panels were taken during a different thruster start-up. There was a gradual emission change in the first two of the three frequencies studied with the Zspan instrument similar to that seen in the LSCX data.

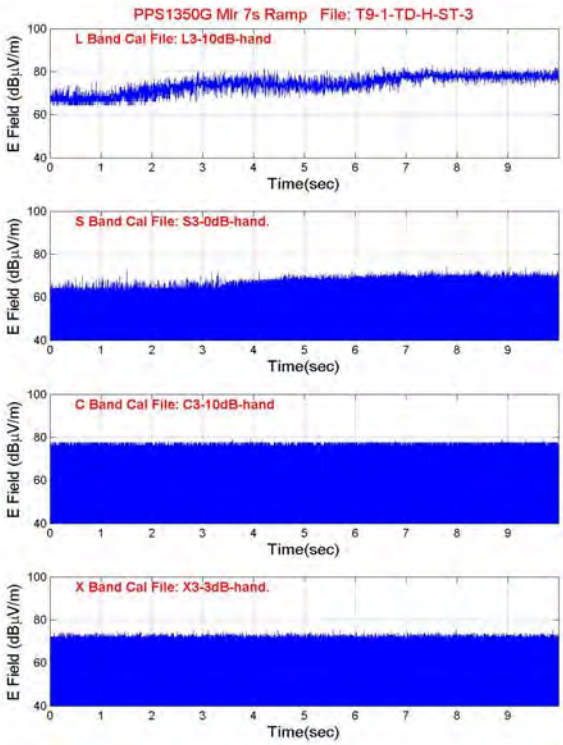

Figure 13 Log plots of horizontally polarized emission from the PPS1350 MIr thruster during a 100V increase in anode potential.

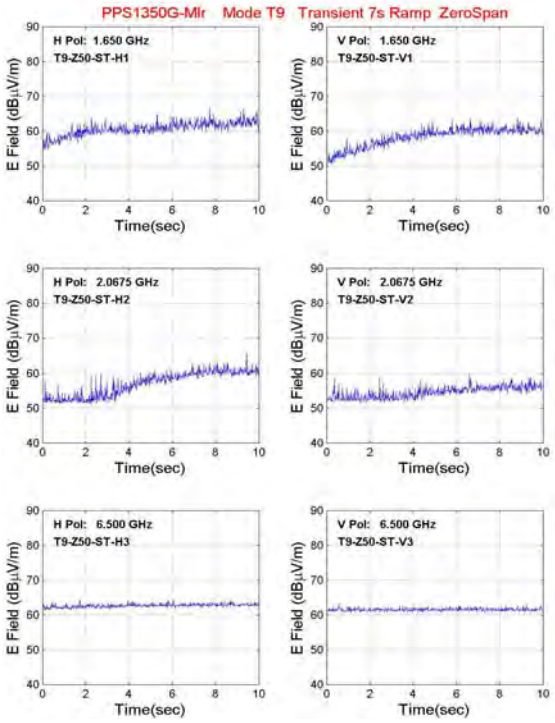

Figure 14 Log plots of Zspan instrument data from the PPS1350 MIr thruster during an 100V increase in anode potential.

V. Summary and Conclusions

The radiated EMI characterization was the final step in the qualification program of the PPS1350-G HET. Two thrusters with significant differences in total operating hours were characterized. The EM thruster having approximately 200 hours and 100 cycles, being an almost new (BOL) thruster. However, the MIr thruster having accumulated roughly 5800 cycles and 6500 hours of accumulated running after this test campaign, can be considered being at the other extreme of the life cycle (EOL). Overall, the emissions observed from the two PPS1350-G HETs were surprisingly low with respect to expectations, based on experiences with similar Hall Effect Thrusters.

As presented in this paper, the measurements performed on the two PPS1350-G thrusters accomplished important goals. First, a deeper insight was gained into the behavior of the radiated emission during all operational phases of the thruster cycle. Second, a large data set was recorded both for conducted and radiated emissions, which when processed will elucidate various physical characteristics of the PPS1350-G. Finally, we note that the radiated emission levels encountered from the two PPS1350-G HETs were surprisingly low in the L-, S-, and C-bands, far lower than first expected based on measurement on very similar thrusters. Generally there are almost no emissions above 2.5 GHz for an end-of-life thruster and limited to more or less 2 GHz for a beginning-of-life thruster, during steady state operational conditions. It is hoped that this last observation will help lead to a deeper understanding the physical origin of this emission.

Acknowledgements

The development of the PPU emulator required the technical assistance of John Nocerino for electronic engineering, Rostislav Spektor for the fault protection and telemetry systems, Timothy Graves for the wiring harness, and Ernest Yohnsee for electronic assembly. The software for the PPU was written by John Nocerino. Kevin Diamant aided in development of the XRFS emulator. Snecma thanks CNES for technical support throughout this campaign. This work was supported by Snecma, CNES, and The Aerospace Corporation Independent Research and Development Program.

References

1. Manzella, D., Sarmiento, C., Sankovic, J., and Haag, T., "Performance Evaluation of the SPT-140," IEPC-97-059, 25th International Electric Propulsion Conference, Cleveland, Ohio, August 1997.

2. Beiting, E. J., Pollard, J.E., Khayms, V., and Werthman, L., "Electromagnetic Emissions to 60 GHz from a BPT-4000 EDM Hall Thruster," IEPC-03-129, 2003 International Electric Propulsion Conference, Toulouse, France, 17-21 March 2003.

3. Beiting, E.J., Garret, M. L., and Pollard, J.E., "Spectral and Temporal Characteristics of Electromagnetic Emissions from the BPT-4000 Hall Thruster," AIAA-2006-5154, 42nd AIAA/ASME/SAE/ASEE Joint Propulsion Conference, Sacramento, CA, July 9-12, 2006.

4. Beiting, E.J., Garret, M. L., and Pollard, J.E., Pezet, B. and Gouvernayre, P., "Spectral Characteristics of Radiated Emission from SPT-100 Hall Thrusters, IEPC2005-221, The International Electric Propulsion Conference, Princeton, NJ, November 2005.

5. Brukhty, V. I. and Kirdyashev, K. O., "Microwave Oscillations as an Indicator of Anomalous Wall Erosion in SPT Accelerating Chamber," IEPC 99-107, 26 International Electric Propulsion Conference, Kitakyushu, Japan, 17-21 October 1999.

6. Marchandise, F.R., Biron, J., Gambon, M., Cornu, N., Darmon, F., Estublier, D., "The PPS®1350 qualification demonstration7500h on ground, about 5000h in flight," IEPC-2005-209, International Electric Propulsion Conference, Princeton, NJ, November 2005.

7. Thompson, R. and Gray, H., "The Xenon Regulator and Feed System For Electric Propulsion Systems," IEPC-2005-066, International Electric Propulsion Conference, Princeton, NJ, November 2005.

8. Beiting, E.J., *Design and Performance of a Facility to Measure Electromagnetic Emissions from Electric Satellite Thrusters*, AIAA-2001-3344, 37th AIAA/ASME/SAE/ASEE Joint Propulsion Conference and Exhibit, Salt Lake City, UT, 8–11 July 2001.

9. Beiting, E.J. and Garret, M. L., "Facility for High-Fidelity Electromagnetic Compatibility Studies of Electric Thrusters," AIAA-2007-5329, 43nd AIAA/ASME/SAE/ASEE Joint Propulsion Conference, Cincinnati, OH, July 8-11, 2007.

10. Tilinin, G. N., "High-frequency plasma waves in a Hall accelerator with an extended acceleration zone," *Soviet Physics, Technical Physics* **22**(8), 974-978, 1977.

11. Choueiri, E. Y., "Plasma Oscillations in Hall Thrusters," *Phys. Plasmas*, **8**(4), 1411-1426 (2001).

12. Kirdyashev, K. P., "Electromagnetic Interference with Hall Thruster Operation," Proc. 4th Int. Spacecraft Propulsion Conf., Cagliari, Sardinia, Italy, 2-4 June 2004 (EAS SP-555), Oct. 2004.

13. Beiting, E.J., Garrett, M. L., Pollard, J.E., Pezet, B., and Gouvernayre, P., "Temporal Characteristics of Radiated Emission from SPT-100 Hall Thrusters in the L- S-, and C-Bands, IEPC2005-222, The International Electric Propulsion Conference, Princeton, NJ, 31 Oct - 4 Nov, 2005.

14. Beiting, E.J., Spektor, R. and Garrett, M.L.,"Experimental Investigation on the Origin of the 1 – 8 GHz Radiated Emission from Hall Thrusters," ISPC-2008-070, Crete, Greece 2008.

15. Beiting, E.J., Spektor, R. and Eapen, X.L, "On the origin of the L-, S- and C-bands (1 – 8 GHz) Emission from Hall Thrusters," IEPC-2009-072, The International Electric Propulsion Conference, Ann Arbor, MI, September 2009.